

Supporting Information

Softness of Atherogenic Lipoproteins: A Comparison of Very Low Density Lipoprotein (VLDL) and Low Density Lipoprotein (LDL) Using Elastic Incoherent Neutron Scattering (EINS)

*Christian Mikl[†], Judith Peters^{‡,||,⊥}, Marcus Trapp[‡], Karin Kornmueller[†], Wolfgang J. Schneider[§]
and Ruth Prassl^{†,*}*

[†]Institute of Biophysics and Nanosystems Research, Austrian Academy of Sciences, Graz, Austria,

[‡]Institut de Biologie Structurale, Grenoble, France

[⊥]Institut Laue Langevin, Grenoble, France

[⊥]Université Joseph Fourier Grenoble I, France

[§]Department of Medical Biochemistry, Medical University Vienna,
Max F. Perutz Laboratories, Vienna, Austria

*To whom all correspondence should be addressed.

Mail: Institute of Biophysics and Nanosystems Research, Schmiedlstr. 6, 8042 Graz, Austria.

Email: ruth.prassl@oeaw.ac.at. Phone: +43-316-4120-305. Fax: +43-316-4120-390.

MATERIALS

Preparation of human very low density lipoprotein (VLDL) and low density lipoprotein (LDL)

Human VLDL and LDL were isolated from human plasma, containing 1 mg/ml Na₂EDTA, 0.083% gentamycin sulfate, and a protease inhibitor cocktail (Roche Diagnostics, Mannheim, Germany), by several steps of ultracentrifugation (200k rcf, 24h, 4°C), starting at its own density and then adjusting the density to 1.063 g/ml by addition of solid potassium bromide (KBr) as described previously.¹ Once isolated, the samples were extensively dialyzed against standard buffer (10 mM Tris, pH 7.4) and concentrated with Amicon Ultra-15 centrifugal filter units (cut-off 100 kDa; Millipore, Billerica, MA) again to reduce the solute to a minimum to facilitate the lyophilisation procedure and promote the neutron scattering measurements.

Preparation of chicken egg yolk VLDL

VLDL from chicken egg yolk was isolated by a modified procedure according to Nimpf et al.² Briefly, yolk from freshly laid hen's egg was thoroughly washed with ice-cold saline and mixed with 5 vol of buffer (20mM Tris, 150 mM NaCl, 0.2 mM EDTA, pH 7.4). For preventing microbial degradation, 1mM PMSF and 5µM Leupeptin were added. The suspension was ultracentrifuged at 150k rcf, 12h at 4°C and the buoyant waxy part on the top was resuspended in 10 vol of buffer and ultracentrifuged again. Aggregates were removed by filtration through a 0.22 µm syringe filter (Roth, Karlsruhe, Germany). Several steps of centrifugation and resuspending in standard buffer (10 mM Tris, pH 7.4) were carried out to confirm the purity of the samples.

Lyophilisation and rehydration

Samples with or without 10% (w/v) sucrose were shock-frozen in liquid nitrogen. Lyophilisation was performed with a Christ Alpha 1-4 LSC freeze dryer (Christ, Osterode, Germany) using a vacuum of 100 Pa for 24 h. To remove residual water (checked by weighing) the samples were put in an exsiccator filled with silica gel, subsequently replaced by phosphorus pentoxide. Rehydration was carried out in D₂O-atmosphere to a level of 0.4 mg D₂O / mg protein. For the sucrose-containing samples, 0.2 mg D₂O / mg sucrose were also added.

Chemical Analysis

Enzymatic assay kits were used to determine the concentrations of protein (BCA protein assay kit; Pierce, Rockford, IL), phospholipids (DiaSys, Holzheim, Germany), total cholesterol (Roche Diagnostics, Mannheim, Germany), free cholesterol (Wako, Neuss, Germany) and triglycerides (bioMerieux, Marcy l'Etoile, France). Cholesteryl ester content was calculated as (total cholesterol – free cholesterol) x 1.68. This factor represents the ratio of the average molecular weight of cholesteryl ester to free cholesterol. The chemical compositions are shown in Table S1.

The purity and homogeneity of the samples were tested by SDS-PAGE (see Figure S1).

Spin-Label ESR Spectroscopy

Spin label analogs of fatty acid (12DSA; 12-doxy-stearic acid; 2-(10-carboxydecyl)-2-hexyl-4,4-dimethyl-3-oxazolidinyloxy) and fatty acid methyl ester (12DSA-ME; 12-doxy-stearic acid methyl ester; 2-(10-methoxycarbonyl-decyl)-2-hexyl-4,4-dimethyl-3-oxazolidinyloxy) were purchased from Sigma-Aldrich (Vienna,

Austria), respectively. Adequate amounts of spin labels were dissolved in ethanol to reach a final concentration of at least 10^{-4} molar during measurements and dried at the walls of a glass vial using a stream of nitrogen. Lipoprotein solutions were concentrated with Vivaspin 2 centrifugal filter units (cut-off 300 kDa; Sartorius, Goettingen, Germany) to achieve a final lipid to label ratio of 100:1 (mol/mol). The reference base for 12DSA was the phospholipid content, and for 12DSA-ME the sum of cholesteryl ester and triglycerides. The respective lipoprotein solutions were added into the vials and gently stirred under argon atmosphere for 2 hours to allow for a complete incorporation or encapsulation of the spin label into the particles.

METHODS

Elastic incoherent neutron scattering (EINS)

The dry powder samples were rehydrated in a D₂O atmosphere to cover the protein surface with a single layer of heavy water molecules in order to allow for anharmonic motions above the dynamical transition temperature.³ A typical sample weight of ~200 mg was put in a flat aluminium sample holder (with dimensions of 30 × 40 × 0.3 mm), which was sealed with an indium ring for tightness. A glove-box was used while loading the sample holder to conserve the exact amount of D₂O in the samples. The weight of the filled sample holder was checked before and after measurements to ensure adequate packing of the samples. No losses were detected for any sample.

Experiments were performed on the thermal neutron backscattering spectrometer CRG-IN13, which is situated at the high flux research reactor ILL (Institute Laue-Langevin, Grenoble, France). The spectrometer provides an energy resolution of 8 μeV (FWHM) for an incident wavelength of 2.23 Å. The detectors cover a Q -range between $0.2 \text{ \AA}^{-1} \leq Q \leq 4.9 \text{ \AA}^{-1}$. The sample-holder was aligned at 135° with respect to the direction of the incident neutron beam. The samples were measured elastically in a temperature range of 20 K to 310 K, in steps of 20 K. In a typical data collection procedure, each point of temperature was measured for 1 hour. In regions of putative dynamical transitions the step width was reduced to either 10 K or 5 K to improve the data resolution. At higher temperatures the increasing error of measurement was compensated by prolonged time of data accumulation.

For analysing the data the standard program LAMP provided by ILL was used.⁴ The transmission of the samples accounted for 0.85 to 0.90, thus multiple scattering could be disregarded. All data were corrected for the background (empty cell) and the transmission of the sample. Each Q -value was normalized by the lowest temperature data point (20 K), where molecular motions are strongly reduced.

The elastic scattering function $S(Q, 0 \pm \Delta E)$ can be simplified within the Gaussian approximation⁵ assuming that the distribution of the atoms around their average position follows a Gaussian distribution, to

$$S(Q, 0 \pm \Delta E) \approx \exp\left(-\frac{1}{6}Q^2 \langle u^2 \rangle\right) \quad (1)$$

where $\langle u^2 \rangle$ are the average atomic mean-square displacements (MSD). This corresponds mainly to the so-called Debye-Waller factor. As Q approaches zero, the approximation is strictly valid for any motion localized in the length-time window of the spectrometer, but it holds up to $\langle u^2 \rangle Q^2 \approx 2$.⁵ The MSD values can be obtained for each temperature point from the slope of the logarithm of the scattered intensities $I(Q)$ according to

$$\langle u^2 \rangle = -6 \frac{d \ln S(Q, 0 \pm \Delta E)}{dQ^2}. \quad (2)$$

Regarding the fact that values of $I(Q)$ become more fluctuating at increasing scattering vectors only data points in the Q -range of $0.27 \text{ \AA}^{-2} \leq Q^2 \leq 4.26 \text{ \AA}^{-2}$ were used in further calculations (see Figure S2). Linear fits applying errors as weights (obtained in the computations before) were performed with *Origin 7* (OriginLab, Northampton, MA). This also assigned to each point a weighted statistical error. The mean-square displacement $\langle u^2 \rangle$ is consistent with the full amplitude of atomic displacement and can be described for each temperature point.

The slope in the plot of local MSD-values vs. T corresponds to an effective mean force constant, written as $\langle k \rangle$, which expresses well the resilience of the system for the motion.⁶

$$\langle k \rangle = 0.00276 / \left(\frac{d \langle u^2 \rangle}{dT} \right) \quad (3)$$

Thus, in biological terms, MSD-values can be associated with flexibility, while the $\langle k \rangle$ -values are a measure for the structural resilience of the system. For the anharmonic regime the resilience can be expressed in terms of pseudo-force constants $\langle k' \rangle$ above the first and $\langle k'' \rangle$ after the second dynamical transition which include the anharmonic dynamics. They are calculated in a quasi-harmonic approach according to Equation 3.⁶ A comparative list of all effective mean force constants from calculations and literature is shown in Table S2.

Electron spin resonance (ESR)

Two different nitroxide spin labels were used to determine the mobility in the phospholipid and core domains of the lipoproteins. Particular focus was put on differences in the mobility of the lipids between samples containing 10% (w/v) sucrose or not. 12DSA was selected because of its ability to incorporate into the surface monolayer with its carboxyl function anchored adjacent to the phospholipid head group. The fatty acid harbors one free radical function at the C-12 position which is most sensitive for mobility changes in the acyl chain region of the phospholipid monolayer in LDL⁷ and hence for VLDL as well. The apolar spin label 12DSA-ME is distributed in the neutral lipid core made up of cholesterol ester and triglycerides.

All ESR experiments were performed on a Bruker ECS106 spectrometer (Bruker, Rheinstetten, Germany) at 9.52 GHz. The modulation frequency was 50 kHz, scan width 200 G, modulation amplitude 2 G and microwave power ~5 mW. Scans involved with the spin label 12DSA show hyperfine splittings typical for anisotropic motion, whereas scans with 12DSA-ME result in splittings specific for rapid, close to isotropic motion. In all scans $2A_{\parallel}$ and $2A_{\perp}$ - referring to the outer and inner hyperfine splitting parameters - were determined, and the fluidity was calculated according to established methods.⁸ In triglyceride-rich regions like the core domain, especially in VLDL particles, the fluidity is very high, reflected as a rapid, isotropic tumbling rate of the nitroxide probe. As a result the determination of the anisotropic hyperfine splitting parameters $2A_{\parallel}$ and $2A_{\perp}$ is difficult. In this case the rotational correlation time τ_c can be calculated according to Kivelson.⁹

$$\tau_c = (6.5 \times 10^{-10}) W_0 \left(\sqrt{\frac{h_0}{h_{-1}}} - 1 \right) \quad (4)$$

W_0 refers to the mid-field line width, h_0 and h_{-1} are the heights of the mid- and high-field lines, respectively. In consequence the rotational correlation time τ_c is used as an additional mobility parameter for scans with nearly isotropic motions.

Photon correlation spectroscopy (PCS)

The particle size of lipoproteins was determined by photon correlation spectroscopy (PCS) with a Zetasizer 3000 HSA (Malvern Instruments, Herrenberg, Germany). The instrument was equipped with a 10 mW helium neon laser

operating at 632.8 nm. The scattered light was detected at an angle of 90° by a photon counting avalanche photodiode detector coupled to a correlator. Particle size was derived by an auto-correlation function. The results are expressed as Z-average, which is the harmonic-intensity averaged particle diameter.

Lipoprotein samples were diluted to a concentration of 0.30 mg/ml (VLDL) and 0.55 mg/mL (LDL) with standard buffer (10 mM Tris, pH 7.4), which was previously filtered through a disposable 0.02 µm membrane filter unit (Anotop 25, Whatman International Ltd., Maidstone, UK). The measurements were performed in 1 cm glass capillaries thermostated at 25°C. To assess the integrity of lipoprotein particles after lyophilisation, the samples were rehydrated, diluted and compared to freshly isolated preparations. The results are summarized in Table S2. We observed no significant difference in the mean particle size for LDL and VLDL samples upon lyophilisation and rehydration. Thus, the particle size data indicate that no aggregation, degradation, or particle fusion occurred.

Table S1. Chemical composition (% per weight) and number fraction (%N_i/N) of hydrogen atoms (¹H) in the individual lipoprotein compounds. As expected the cholesterol portion is highest in hLDL, while triglycerides are more dominant in VLDL¹⁰ with an even lower weight ratio of CE to TG in VLDL from chicken egg yolk (yVLDL).

Compound	Chemical composition(% w/w)			¹ H-fraction (% N _i /N)		
	yVLDL	hVLDL	hLDL	yVLDL	hVLDL	hLDL
Protein	13.2	14.2	22.6	8.5	9.2	15.1
Phospholipid	17.2	17.0	21.9	16.9	17.0	22.5
Cholesterol, free	2.7	5.9	8.5	3.0	6.4	9.5
Cholesterol, esterified	0.3	7.7	43.9	0.4	8.4	49.3
Triglycerides	66.6	55.1	3.2	71.2	59.1	3.5

y, yolk; h, human; LDL, low density lipoprotein; VLDL, very low density lipoprotein; N_i, number of hydrogen atoms in the individual lipoprotein compound; N, total number of hydrogens.

Table S2 : Particle size distribution determined by PCS. The mean particle sizes of freshly prepared human LDL and VLDL are compared to lyophilized and rehydrated LDL and VLDL samples, respectively.

Sample	ZAve (nm)	SD (+/-)
LDL	38.6	1.7
LDL lyo	36.5	0.7
VLDL	53.9	0.5
VLDL lyo	53.7	0.9

lyo, lyophilized and rehydrated lipoproteins; ZAve, mean hydrodynamic diameter (nm). PCS-data are expressed as means ± SD (n=3). For the statistic evaluation a two-sample Student-t-test was used. No statistically significant differences were observed between different LDL or VLDL samples. Statistical significance was assumed at p<0.05. Statistics were performed using the program MINITAB 13.31 (MiniTab Inc.).

Table S3. List of effective mean force constants [N/m] achieved from calculations and literature.^{6,11-13}

Sample	<k>	<k'>	<k''>
hLDL sucrose	1.96	0.7	0.25
yVLDL sucrose	1.62	0.39	0.21
hLDL	1.21	0.32	0.16
yVLDL	0.97	0.20	0.061
hVLDL	0.77	0.17	0.066
Mb trehalose ¹¹	-	-	3
Mb ¹²	2	-	0.3
PM labeled ⁶	1.4	-	0.33
PM ⁶	1.7	0.55	0.12
Hb ¹³	1.18	-	0.17

Hb, hemoglobin; Mb, myoglobin; PM, purple membrane; labeled, only Retinal, Trp and Met residues of PM were hydrogenated; <k>, <k'>, <k''> effective mean force constants for different temperature regions subdivided by dynamical transitions. Here, for comparison, <k''> corresponds to the area of physiological temperatures.

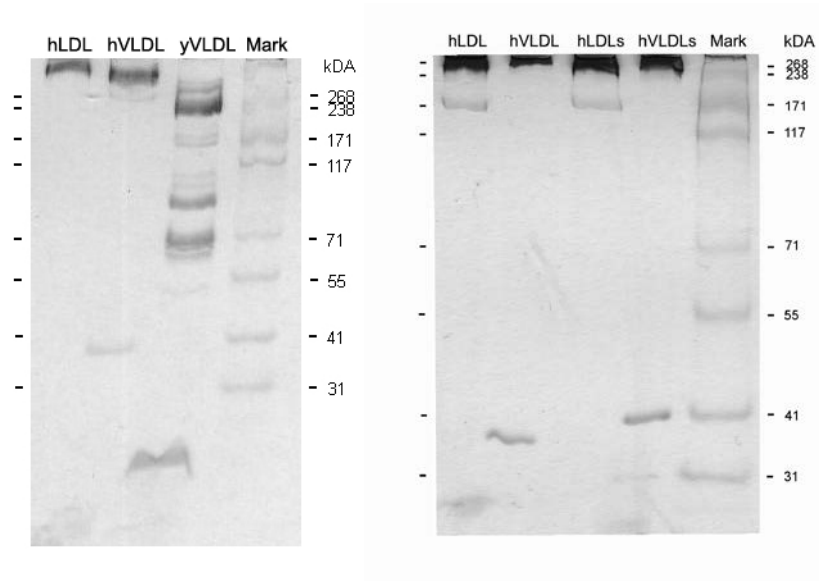


Figure S1. SDS-PAGE gel (4.5 - 18%) of LDL and VLDL from human plasma and chicken egg yolk

h, human; y, yolk; s, sucrose added (10% w/v); LDL, low density lipoprotein; VLDL, very low density lipoprotein; Mark, pre-stained high molecular weight standard (Invitrogen). As seen on the gel (left side) hLDL harbors only one major apolipoprotein, namely apoB100. hVLDL exhibits apoB100, but also some small exchangeable apolipoproteins, mainly apoC and apoE. yVLDL comprises apoB100 in a proteolytically cleaved form, and also harbors apoVLDL-II (the fastest migrating band). For comparison (right side) the gel for human LDL and VLDL after lyophilization and rehydration are shown. There are no substantial differences observed before and after lyophilization neither for samples with nor without sucrose. This indicates that apoB100 is not degraded during lyophilisation.

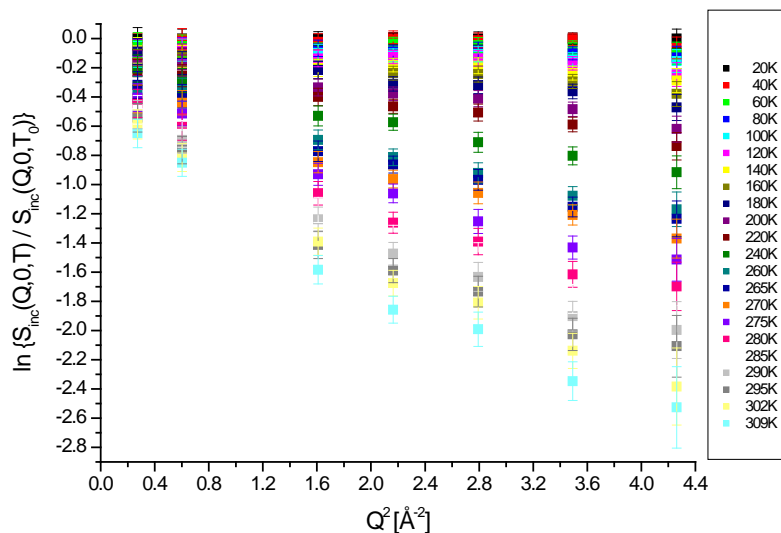


Figure S2 (A). Dependence of the elastic neutron scattering intensities $S(Q,0 \pm \Delta E)$ from the scattering vectors (Q^2) shown for hVLDL at different temperatures. The given Q -range was used for following calculations and reflects the inner regime of the scattering intensities.

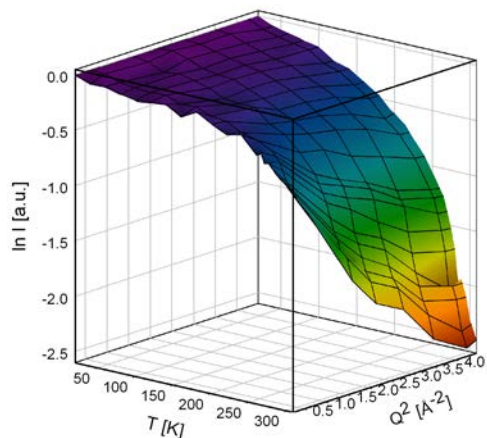


Figure S2 (B). As representative example, the three dimensional plot of hVLDL shows the dependence of elastic neutron scattering intensities $I(Q)$ from the scattering vectors (Q^2) as a function of temperature T . The chosen Q -range displayed here guarantees linearity of the data and allows for calculations of MSD values.

Reference List

- (1) Johs, A.; Hammel, M.; Waldner, I.; May, R. P.; Laggner, P.; Prassl, R. *J.Biol.Chem.* **2006**, *281*, 19732-19739.
- (2) Nimpf, J.; Radosavljevic, M.; Schneider, W. J. *Proc.Natl.Acad.Sci.U.S.A* **1989**, *86*, 906-910.
- (3) Rupley, J. A.; Careri, G. *Adv.Protein Chem.* **1991**, *41*, 37-172.
- (4) LAMP, the Large Array Manipulation Program. **2010**.
Computer Program
- (5) Gabel, F.; Bicout, D.; Lehnert, U.; Tehei, M.; Weik, M.; Zaccai, G. *Q.Rev.Biophys.* **2002**, *35*, 327-367.
- (6) Zaccai, G. *Science* **2000**, *288*, 1604-1607.
- (7) Laggner, P.; Kostner, G. M. *Eur.J.Biochem.* **1978**, *84*, 227-232.
- (8) Seelig, J. Anisotropic Motion in Liquid Crystalline Structures; In *Spin Labeling Theory and Applications*; Berliner, L. J., ed. Academic Press: New York, San Francisco, London, **1976**; pp 373-409.
- (9) Kivelson, D. *J.Chem.Phys.* **1960**, *33*, 1094-1107.
- (10) Hegele, R. A. *Nat.Rev.Genet.* **2009**, *10*, 109-121.
- (11) Cordone, L.; Ferrand, M.; Vitrano, E.; Zaccai, G. *Biophys.J.* **1999**, *76*, 1043-1047.
- (12) Doster, W.; Cusack, S.; Petry, W. *Nature* **1989**, *337*, 754-756.
- (13) Stadler, A. M.; Digel, I.; Embs, J. P.; Unruh, T.; Tehei, M.; Zaccai, G.; Buldt, G.; Artmann, G. M. *Biophys J* **2009**, *96*, 5073-5081.